Original Research

Gadolinium-Enhanced, Vessel-Tracking, Two-Dimensional Coronary MR Angiography: Single-Dose Arterial-Phase vs. Delayed-Phase Imaging

Vincent B. Ho, MD,[1,2]* Thomas K. F. Foo, PhD,[3] Andrew E. Arai, MD,[2] and Steven D. Wolff, MD, PhD[2]

The purposes of our study were to investigate the benefits of using a single dose of an extracellular contrast agent for coronary magnetic resonance angiography (CMRA) and to determine the relative benefits of arterial-phase vs. delayed-phase image acquisition. The right coronary artery was imaged in 10 healthy adults using a breath-hold, two-dimensional fast gradient echo pulse sequence designed for vessel tracking (multiphase, multislice image acquisition). Pre- and postcontrast CMRA was performed. Postcontrast imaging consisted of arterial- and delayed-phase CMRA following a 15 mL bolus (single dose) of contrast media and of delayed-phase imaging following a cumulative 45 mL contrast dose (triple dose). Contrast-enhanced CMRA provided a significantly higher ($P < 0.001$) signal-to-noise ratio (SNR) and contrast-to-noise ratio (CNR) than noncontrast CMRA. CNR was highest for single-dose arterial-phase CMRA (13.1 ± 4.5) and triple-dose delayed-phase CMRA (13.0 ± 4.8), followed by single-dose delayed-phase CMRA (8.4 ± 3.5) and noncontrast CMRA (4.2 ± 1.8). Single-dose arterial-phase CMRA provided the best visualization of the distal right coronary artery and was preferred for blinded physician assessments. We concluded that utilization of a single dose of extracellular contrast media improves CMRA, especially if timed for arterial-phase imaging. J. Magn. Reson. Imaging 2001;13: 682–689. © 2001 Wiley-Liss, Inc.

Index terms: coronary vessels, MR; magnetic resonance, vascular studies; gadolinium; arteries, MR; arteries, coronary; magnetic resonance, contrast enhancement

ARTERIAL-PHASE GADOLINIUM (Gd)-enhanced magnetic resonance angiography (MRA) has been shown to be a reliable and quick method for imaging arteries, such as the aorta and its branches (1–5), the pulmonary arteries (6), and the carotid arteries (7). Unlike other MRA methods, Gd-enhanced MRA relies primarily on the T1 shortening of blood by contrast media and generates "luminograms," which resemble conventional x-ray angiograms. As with conventional angiography, selective arterial visualization is achieved by the collection of imaging data (notably, the low-spatial frequency data or the time domain data about the center of k-space) during the arterial transit of the contrast media bolus.

The coordination of the imaging with arterial enhancement optimizes both arterial signal and arterial depiction (4,7–10). Timing of arterial-phase imaging can be accomplished using several methods. One common technique is to perform a preliminary timing bolus scan (4,8,9) to estimate time of contrast arrival. Another common method is to employ an automated bolus detection algorithm (7,10) that can detect contrast arrival in real time and initiate imaging for the arterial phase. With either method, proper coordination of central k-space data acquisition with arterial enhancement optimizes the arterial signal and can lower the contrast media dose requirement (9).

Recently, Goldfarb and Edelman (11) and Kessler et al. (12) have described the feasibility of using standard extracellular Gd-chelate contrast agents for breath-hold coronary MRA (CMRA). In both studies, circulatory times for arterial imaging were estimated by a preparatory test bolus scan, and 20–40 mL of contrast was hand injected over 20–25 seconds for the MRA. Image acquisition was performed in the axial plane and targeted the proximal coronary arterial trees. The right coronary artery (RCA), which is better visualized in the double-oblique plane (13), was not imaged in roughly a quarter of the subjects (3 of 13 subjects (12)) and, when seen, only depicted for roughly 4 cm (12). Both investigations, furthermore, studied only the initial postcontrast CMRA acquisition.

In our study, the temporal benefits (arterial vs. delayed phase) of using a single dose (15 mL) of an extra-

[1]Department of Radiology, Uniformed Services University of the Health Sciences, Bethesda, Maryland.

[2]Laboratory of Cardiac Energetics, National Heart, Lung and Blood Institute, National Institutes of Health, Bethesda, Maryland.

[3]Applied Science Laboratory, General Electric Medical Systems, Milwaukee, Wisconsin.

The opinions or assertions contained herein are the private views of the authors and are not to be construed as official or reflecting the views of the Department of Defense or the Uniformed Services University of the Health Sciences.

Steven D. Wolff's current address is Lenox Hill Vascular and Heart Institute, New York, NY.

*Address reprint requests to: V.B.H., Department of Radiology, Uniformed Services University, 4301 Jones Bridge Road, Bethesda, MD 20814-4799. E-mail: vho@usuhs.mil

Received August 18, 2000; Accepted October 30, 2000.

cellular contrast agent for coronary imaging were studied. Imaging consisted of four separate breath-hold CMRA acquisitions: noncontrast, single-dose arterial phase, single-dose delayed phase, and triple-dose (cumulative 45 mL) delayed phase. The single-dose and triple-dose delayed-phase CMRA served as relative comparisons for the benefits of arterial-phase CMRA. The higher dose delayed-phase CMRA was also included because it was recognized that CMRA could potentially have a role as part of an integrated contrast-enhanced cardiovascular study (i.e., "one-stop-shop" concept for cardiovascular MR). For example, CMRA may serve as a supplement to a stress and rest myocardial perfusion study or an atherosclerosis evaluation that included several Gd-enhanced MRA acquisitions. In these cases, CMRA would follow these other primary applications, for which higher cumulative contrast media doses may have already been administered.

For the purposes of this pilot investigation, imaging of a single coronary artery was deemed sufficient to investigate the advantages of single-dose arterial-phase CMRA over those of delayed-phase imaging following the single and higher doses. Focusing on a single vessel ensured reproducibility of CMRA localization between acquisitions, as well as minimized the time interval between each breath-hold acquisition. The RCA was chosen because its relative planar orientation within the right atrioventricular groove was well suited for its visualization on a two-dimensional (2D) CMRA, thereby enabling better assessment of arterial length improvements from the use of contrast media. Each CMRA was performed using vessel tracking (14), a multislice technique that acquires images throughout the cardiac cycle (i.e., during both systole and diastole).

MATERIALS AND METHODS

All experiments were performed with the approval of the Institutional Review Board and in accordance with institutional regulations on the use of human subjects. Informed consent was obtained in the 10 healthy volunteers (8 men and 2 women) who ranged in age from 21 to 58 years (mean age = 36.4 ± 11.6 years) and in weight from 66 to 113 kg (mean weight = 82.3 ± 13.7 kg). All examinations were performed on a 1.5 Tesla MR imaging (MRI) system (Signa version 5.5, General Electric Medical Systems, Waukesha, WI) with a prototype high-performance gradient subsystem capable of achieving a maximum gradient amplitude of 40 mT/m. Imaging was performed using a cardiac phased-array coil.

The RCA was localized in the appropriate double-oblique plane, using a series of breath-hold axial and oblique-electrocardiogram (ECG)-gated fast 2D-segmented k-space gradient echo pulse sequences (FASTCARD; repetition time (TR)/echo time (TE), 9.5–10 msec/2.3 msec; flip angle, 30°; eight views per segment; one excitation; 256 × 224 matrix). The oblique 2D FASTCARD images were performed in a multiphase, single-slice "cine" mode and were used both to guide the prescription of the optimum double-oblique plane for RCA visualization and to determine the maximum anatomic excursion of the RCA over the cardiac cycle.

Each CMRA acquisition was performed using an ECG-gated vessel-tracking pulse sequence (14) that adjusts the slice location based on the anticipated location of the RCA during each specific cardiac phase. The end-systolic and end-diastolic locations, as displayed on the initial oblique 2D FASTCARD localizer, were used as the limits of the double-oblique spatial excursion of the vessel-tracking CMRA acquisition. The vessel-tracking method has been shown to roughly triple the percentage of images that the coronary artery is visualized during a breath-hold 2D CMRA (14). In this manner, vessel tracking improves the overall imaging efficiency of each breath-hold acquisition, enabling the illustration of substantial lengths of the coronary artery during a single breath-hold acquisition.

Once the ideal double-oblique plane and vessel-tracking parameters were determined for the initial noncontrast CMRA, all subsequent contrast-enhanced CMRA studies were performed with identical scan parameters. In order to further minimize spatial differences between CMRA acquisitions, each CMRA acquisition was obtained during a single breath hold during end expiration and the time between CMRA acquisitions was kept to a minimum.

All CMRAs were performed using an ECG-gated vessel-tracking fat-suppressed fast 2D-segmented k-space gradient echo pulse sequence (FCARDVT; TR/TE, 9.5–10 msec/2.3 msec; flip angle, 30°; eight views per segment; one excitation). The images were radio-frequency phase spoiled and were obtained with a 28–32 cm field of view (FOV), 5-mm slices, receiver bandwidth of ±16 kHz, 256 × 224 matrix (1.1–1.4 mm/pixel in-plane resolution), and a 0.75 asymmetrical FOV. With eight views or k-space lines per segment (or per R-R interval), CMRA images from 7 to 11 spatial locations were acquired in each acquisition, depending on the subject's heart rate. A localized volume shim was performed on each subject prior to the initial CMRA (i.e., the noncontrast CMRA) and the same transmit and receiver gain settings were used for all subsequent CMRA acquisitions.

An automated contrast bolus detection algorithm (MR SMARTPREP, General Electric Medical Systems, Waukesha, WI) (10,15) was employed to initiate data acquisition of the single-dose arterial-phase Gd-enhanced CMRA. The automated contrast bolus detection technique was prescribed to monitor the signal in a 20 × 20 × 25-mm volume of interest centered within the right ventricle. The right ventricle was selected as it afforded sufficient lead time for proper alignment of central k-space data acquisition with the arterial phase of the contrast bolus. The monitoring phase consisted of a 90–180° spin echo sequence with orthogonal slice-selective gradients and a sequence time (TR) of 25 msec. When the signal intensity in the right ventricle increased beyond two predetermined thresholds (3 SD and 30% above the mean baseline level), the MR pulse sequence switched from the monitoring phase to the data acquisition phase.

Once the thresholds were exceeded, MR SMARTPREP triggered the initiation of a fat-suppressed, vessel-tracking 2D CMRA acquisition. The triggering of the data acquisition phase produced an audible change in

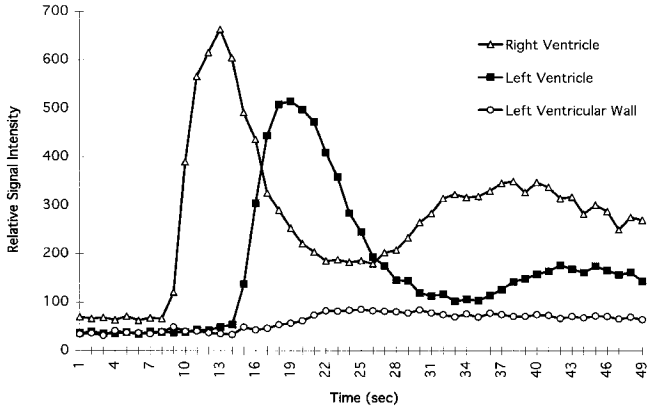

Figure 1. Contrast enhancement vs. time. This signal intensity–time plot shows the relative enhancement patterns of the right ventricle, left ventricle, and left ventricular wall in a normal volunteer following the bolus infusion of 10 mL of gadopentetate dimeglumine. As represented in this scenario, the signal within the right ventricle would exceed a 30% rise in signal threshold (i.e., satisfy the criteria to trigger MR SMARTPREP) at approximately 8.5 seconds. Using MR SMARTPREP prescribed for a 5-second delay, CMRA data acquisition would be initiated at 13.5 seconds, with the center k-space lines (sequential phase ordering used for CMRA) being acquired at 21–25 seconds, synchronized with peak enhancement of the coronary arteries and myocardium.

the gradient noise. The change in gradient noise provided a cue for the volunteer to initiate a 15–22-second breath hold (actual time depending on individual heart rate). The delay between the trigger (i.e., time that both thresholds were exceeded) and the initiation of the actual CMRA acquisition was set for 5 seconds. Fives seconds was chosen based on the estimated transit time (Fig. 1) of contrast from within the right ventricle, through the pulmonary circulation, the left ventricle, the aorta, and into the coronary arteries. In addition, it afforded sufficient time for the patient to initiate a breath hold. During this 5-second delay interval between the end of the monitoring phase and the start of actual data acquisition, dummy radio-frequency excitations were played out to establish a magnetization steady state. This scheme allowed the subjects to maximize the efficiency of their breath holding by requiring them to hold their breath only during the actual image data acquisition period.

In all subjects, noncontrast CMRA was performed with MR SMARTPREP. The algorithm was programmed for a 50-second fail-safe monitoring period, after which the data acquisition phase was automatically begun despite the absence of a detectable rise in the monitoring volume signal. This trial run allowed the volunteers to familiarize themselves with the change in gradient noise, the cue for them to initiate their breath holding.

Following the noncontrast CMRA, arterial-phase Gd-enhanced CMRA was performed using MR SMARTPREP in conjunction with an intravenous bolus of 15 mL (single dose) of gadopentetate dimeglumine (Magnevist, Berlex Laboratories, Wayne, NJ; 0.07–0.11 mmol/kg). In all cases, the MR SMARTPREP triggered successfully prior to the expiration of the 50-second monitoring period. Within 1–2 minutes of the end of the arterial-phase CMRA, another breath-hold CMRA (single-dose delayed-phase CMRA) was acquired at the same scan locations, however, without additional contrast media and without MR SMARTPREP. Approximately 2 minutes following the intravenous infusion of another 30 mL of gadopentetate dimeglumine for a cumulative dose of 45 mL (triple dose, 0.20–0.34 mmol/kg), a final untimed CMRA (triple-dose delayed-phase CMRA) was performed in all but one subject (in this case, secondary to time constraints). All contrast media injections were performed at a rate of 3 mL/second and were followed by a 15-mL saline flush (also at a rate of 3 mL/second) using an MR-compatible injector (Spectris, Medrad Inc., Indianola, PA).

Signal measurements from images were obtained using an operator-defined region of interest (Fig. 2) on an independent computer console. Measurements were obtained from the same phase of the cardiac cycle for each subject. The signal within the proximal RCA (initial 5 cm of the RCA), adjacent tissue (primarily fat in the atrioventricular groove), and artifact-free air outside the thorax were measured. The SD of the signal measurement of air outside the body was used as a measure of image noise. RCA signal-to-noise ratio (SNR) and contrast-to-noise ratio (CNR) were calculated for each acquisition. SNR was defined as the proximal RCA signal measurement divided by image noise. CNR was defined as the signal difference between the proximal RCA and adjacent tissue divided by noise.

To assess each technique's ability to illustrate the distal RCA, the length of the RCA visualized on each breath-hold CMRA acquisition was measured on an independent computer workstation. The vessel-tracking algorithm, by improving the number of images that the RCA was visualized, facilitated the identification of

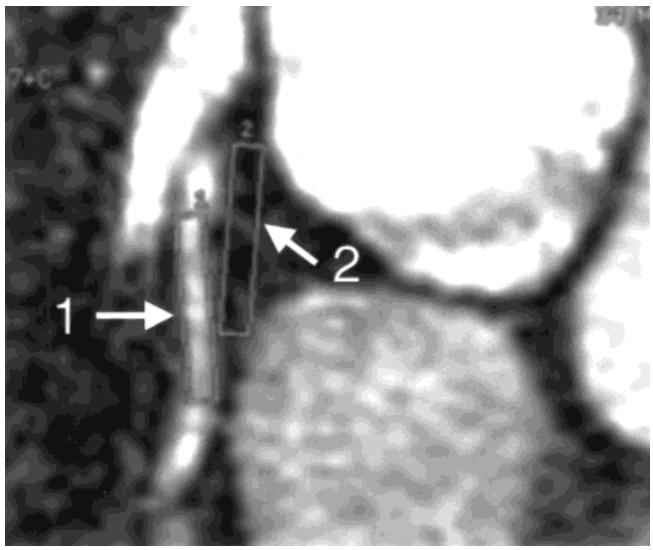

Figure 2. Source image from an arterial-phase vessel-tracking 2D CMRA demonstrating the regions of interest used to measure signal within the proximal RCA (1) and the adjacent tissue (2). The difference in the signal intensities was divided by the SD of artifact-free air measured external to the thorax (not shown) to yield the arterial CNR.

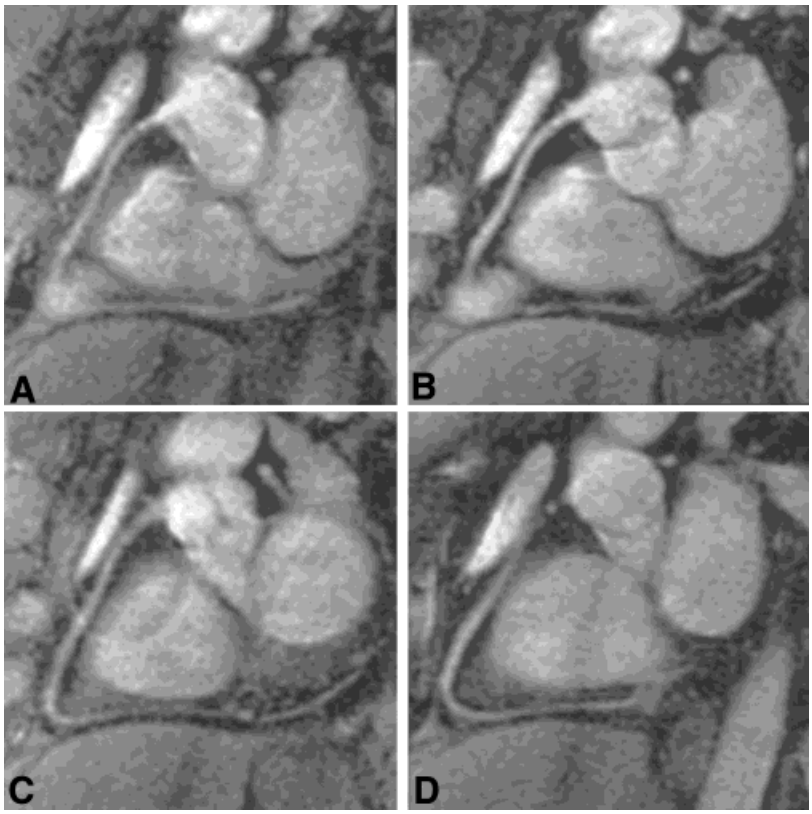

Figure 3. A substantial length of the RCA was illustrated on the single-dose arterial-phase vessel-tracking 2D CMRA (**a–d**) (four of eight images from the CMRA acquisition). The vessel-tracking algorithm provides a greater number of images of the RCA, thereby facilitating visualization of the RCA during a single breath hold. For example, the proximal RCA is not well illustrated on image d but is on images a through c. Likewise, the mid-RCA is not as well visualized on images a and b but is on images c and d. The combination of all the images provides a good depiction of the RCA.

contiguous arterial segments and the measurement of RCA lengths (Fig. 3).

To determine qualitative differences between the various techniques for CMRA, each set of images was evaluated in a blinded fashion by a cardiologist and a radiologist. Reviewers were asked to compare each subject's CMRA studies and rank them in the order of preference for RCA visualization. In the subjects with all four CMRA studies, the ranking was from 1 (best) to 4 (worst).

Analysis of variances and pairwise multiple comparison of SNR, CNR, and RCA length measurements and physician preference was performed using commercially available statistical software (SigmaStat, version 2.0, Jandel Corporation, San Rafael, CA).

RESULTS

The SNR, CNR, and RCA length results are summarized in Table 1. In all subjects, contrast-enhanced CMRA (Fig. 4) provided significantly better ($P < 0.001$) arterial signal (i.e., SNR) and arterial-to-background image contrast (i.e., CNR) than noncontrast CMRA. Compared to noncontrast CMRA, arterial SNR was significantly higher (in descending order) on triple-dose delayed-phase CMRA ($P < 0.001$), single-dose arterial-phase CMRA ($P < 0.001$), and single-dose delayed-phase CMRA ($P = 0.004$). Pairwise multiple comparison revealed a statistically significant difference ($P < 0.05$) between all groups except between single-dose arterial-phase and triple-dose delayed-phase CMRA ($P = 0.093$), and single-dose arterial-phase and single-dose delayed-phase CMRA ($P = 0.23$).

Arterial CNR was statistically higher for single-dose arterial-phase CMRA ($P < 0.001$) and triple-dose delayed-phase CMRA ($P < 0.001$) and single-dose delayed-phase CMRA ($P = 0.012$). Pairwise multiple comparison of the groups revealed that all CNR differences, except that between single-dose arterial-phase CMRA and triple-dose delayed-phase CMRA ($P = 0.98$) were statistically significant ($P < 0.05$). Both single-dose arterial-phase CMRA and triple-dose delayed-phase CMRA provided threefold improvements in RCA image contrast, compared with noncontrast CMRA. The similarity of CNR improvement by both techniques is curious given the slightly higher—albeit not significantly

Table 1
RCA Measurements

	Non-contrast	Single-dose arterial-phase	Single-dose delayed-phase	Triple-dose delayed-phase
SNR	13.9 ± 4.6	23.1 ± 4.8	20.2 ± 4.5	26.5 ± 5.0
CNR	4.3 ± 1.8	13.5 ± 4.6	8.4 ± 3.7	13.0 ± 4.8
RCA length (cm)	6.4 ± 4.0 (6.9 ± 4.8[a])	10.0 ± 4.2 (11.9 ± 3.6[a])	8.2 ± 3.9 (9.4 ± 4.0[a])	7.5 ± 3.6 (8.5 ± 4.0[a])

[a]Measurements excluding the 3 subjects in which only the proximal RCA (initial 5–6 cm) was included within the 2D imaging plane.

higher ($P = 0.093$)—arterial SNR of the triple-dose delayed-phase CMRA. This is attributable to the differences in background signal, which increased over time. Background signal on single-dose arterial-phase CMRA was equivalent to that measured on precontrast CMRA. However, a 22.1% increase in background signal (vs. that on precontrast and single-dose arterial-phase CMRA) was noted on single-dose delayed-phase CMRA, and a 39.9% increase was noted on triple-dose delayed-phase CMRA. One notable additional finding was that single-dose delayed-phase CMRA generated two times the CNR of noncontrast CMRA.

The proximal RCA was visualized in all volunteers with the longest RCA lengths (Table 1), more consistently being visualized on the single-dose arterial-phase CMRA (Fig. 3). On average, shorter lengths of RCA were seen (in descending order) on single-dose delayed-phase CMRA, triple-dose delayed-phase CMRA, and noncontrast CMRA. Pairwise multiple comparison of the groups failed to demonstrate a statistically significant ($P < 0.05$) improvement in RCA length following contrast administration. However, there was a trend for improved visualization of the distal RCA on single-dose arterial-phase CMRA ($P = 0.06$) than on noncontrast CMRA. Delayed-phase acquisitions (single-dose, $P = 0.33$; triple-dose, $P = 0.55$) failed to demonstrate similar improvements over noncontrast CMRA. In three subjects, however, arterial visualization was limited to the proximal RCA (initial 5–6 cm). In these cases, arterial tortuosity prevented the inclusion of the entire RCA (i.e., its distal segments) within the 2D scan plane. In the seven subjects (Table 1) in which the distal RCA was imaged (Fig. 3), there was a statistically significant improvement for single-dose arterial-phase CMRA ($P < 0.05$) but not for the delayed-phase CMRA acquisitions.

Blinded physician evaluation of the examinations demonstrated a statistically significant ($P < 0.05$ for all pairwise comparisons) preference for single-dose arterial-phase CMRA (average rating = 1.5; ranking from 1 to 4) over triple-dose delayed-phase CMRA (average rating = 2.0), single-dose delayed-phase CMRA (average rating = 2.5), and noncontrast CMRA (average rating = 4.0).

DISCUSSION

A variety of MR methods have been suggested for imaging the coronary arteries, including spin density, time-of-flight effect, and T2 signal differences (16–22). None, however, has yet been shown to be reliable for the routine screening and grading of coronary artery disease (11). In this study, extracellular contrast media was found to significantly improve coronary artery illustration. Arterial visualization was best on arterial-phase images. The image contrast (i.e., CNR) improvements of arterial-phase CMRA were equivalent to that of delayed-phase CMRA using three times the contrast media dose. Arterial-phase imaging affords the most efficient use of contrast media dose and diminishes dose requirements for Gd-enhanced CMRA.

Lower contrast dose requirements, aside from their obvious cost benefits, provide additional opportunities to use contrast media for other applications during the same examination. The arterial-phase Gd-enhanced CMRA of one arterial tree, such as the RCA, for example, can be followed by another arterial-phase Gd-enhanced CMRA of another vascular region, such as the left coronary arteries. The second arterial-phase Gd-enhanced CMRA can also be performed successfully using the SMARTPREP algorithm, but a lower trigger threshold (15–20 percent (15)) should be used to account for the elevated baseline arterial signal from the prior dose. However, given the possible twofold increase in CNR on delayed-phase imaging, as shown in our study, the additional administration of contrast media may not be necessary if delayed imaging is promptly performed. Lower dose requirements for Gd-enhanced CMRA also provide the opportunity to use contrast media for an entirely different application—perhaps a myocardial perfusion examination or Gd-enhanced MRA of a different vascular territory.

Compared to noncontrast images, arterial-phase CMRA improved visualization of the distal RCA. This is attributable to Gd-enhanced CMRA's reliance on T1 shortening effects by arriving contrast media, as opposed to in-flow or time-of-flight effects, as in the case of the noncontrast CMRA. On noncontrast CMRA, in-plane saturation probably contributed greatly to the diminished signal and poor depiction of the distal RCA. Admittedly, the vessel-tracking algorithm by imaging roughly the same imaging plane throughout the cardiac cycle probably further saturates arterial signal intensity and may have contributed to the relative poorer illustration of the distal RCA on noncontrast CMRA. However, the average RCA length (6.4 cm) measured on the noncontrast CMRA in our study is comparable to that reported for other 2D CMRA techniques (18–21), where the average RCA length ranged from 5.3 cm (19) to 6.5 cm (20,21). RCA signal intensity was not measured for these other techniques, and thus further comparison is not possible.

Visualization of the distal RCA was not statistically better on the delayed-phase CMRA acquisitions despite their high SNR and high CNR. This may be due to the small number of subjects enrolled in this study, as there was a tendency for the distal RCA to be better seen on the delayed-phase images than on the noncontrast images. The reduction of arterial length visualization on delayed-phase images (vs. arterial phase) most likely resulted from the extravascular leakage of contrast media over time, which, in turn, resulted in increased background signal (22.1% increase on single-dose delayed-phase images; 39.9% increase on triple-dose delayed-phase CMRA). This effect, although noted also in the proximal RCA (Fig. 4), was probably more apparent in the small-caliber distal coronary artery, where there is relatively less surrounding fat and a smaller separation from adjacent enhancing structures, such as the myocardium (Fig. 4). Blinded physician assessment of the techniques agreed with the above CNR and distal RCA observations with single-dose arterial-phase CMRA being most preferred.

The results of our study support those described by Kessler et al. (12) in 13 subjects (2 normal volunteers and 11 patients) and Goldfarb and Edelman (11) in 4 normal volunteers. Kessler et al. reported a 41% higher

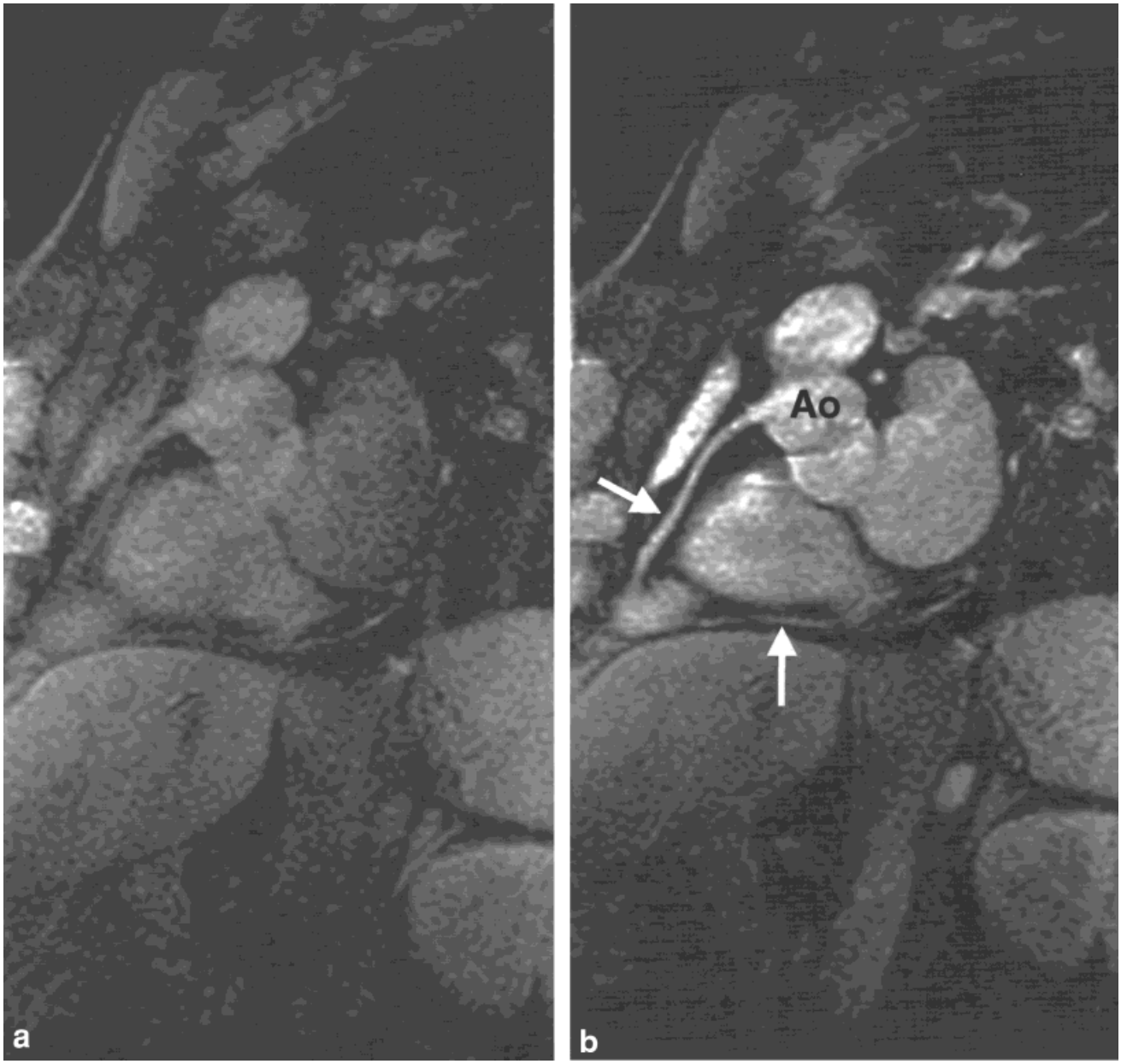

Figure 4. The RCA (**b**) (arrows) was visualized on all CMRA acquisitions. **a:** Noncontrast CMRA; b: single-dose arterial-phase CMRA; **c:** single-dose delayed-phase CMRA; **d:** triple-dose delayed-phase CMRA. However, better RCA illustration was noted following contrast media administration. Note that the blurring of the RCA margins on later delayed-phase images (c–d) when compared with the initial arterial-phase CMRA (b). Ao = aorta.

arterial SNR and a 29% higher arterial CNR with breath-hold Gd-enhanced 3D CMRA than those with noncontrast respiratory-gated 3D CMRA. Goldfarb and Edelman did not measure coronary artery signal per se but reported a 583% improvement in aortic signal using the same pre- and postcontrast axial breath-hold 3D pulse sequence. Our results showed a two- to threefold improvement in RCA image contrast following the use of contrast media. The numerous differences to include CMRA technique, method of signal measurement, contrast dose, rate and method of contrast administration, and timing precludes a sensible comparison of these results. However, all have shown a benefit to the use of extracellular Gd-chelate contrast agents for CMRA.

For this study, the MR SMARTPREP algorithm was modified to monitor a small volume ($20 \times 20 \times 25$ mm), which enabled selective sampling of signal intensity within a specific cardiac chamber. The MR SMARTPREP algorithm provided sufficient temporal resolution (0.5 seconds) for the real-time monitoring of signal intensity in the right ventricle and afforded sufficient lead time for the subjects to initiate end expiratory breath holding. MR SMARTPREP's sampling of the signal is 2–4 times faster than most conventional image-based detection methods (4). Furthermore, despite concurrent respiratory and cardiac motion during the non–breath-hold monitoring phase, the algorithm was able to detect the intraventricular arrival of the contrast

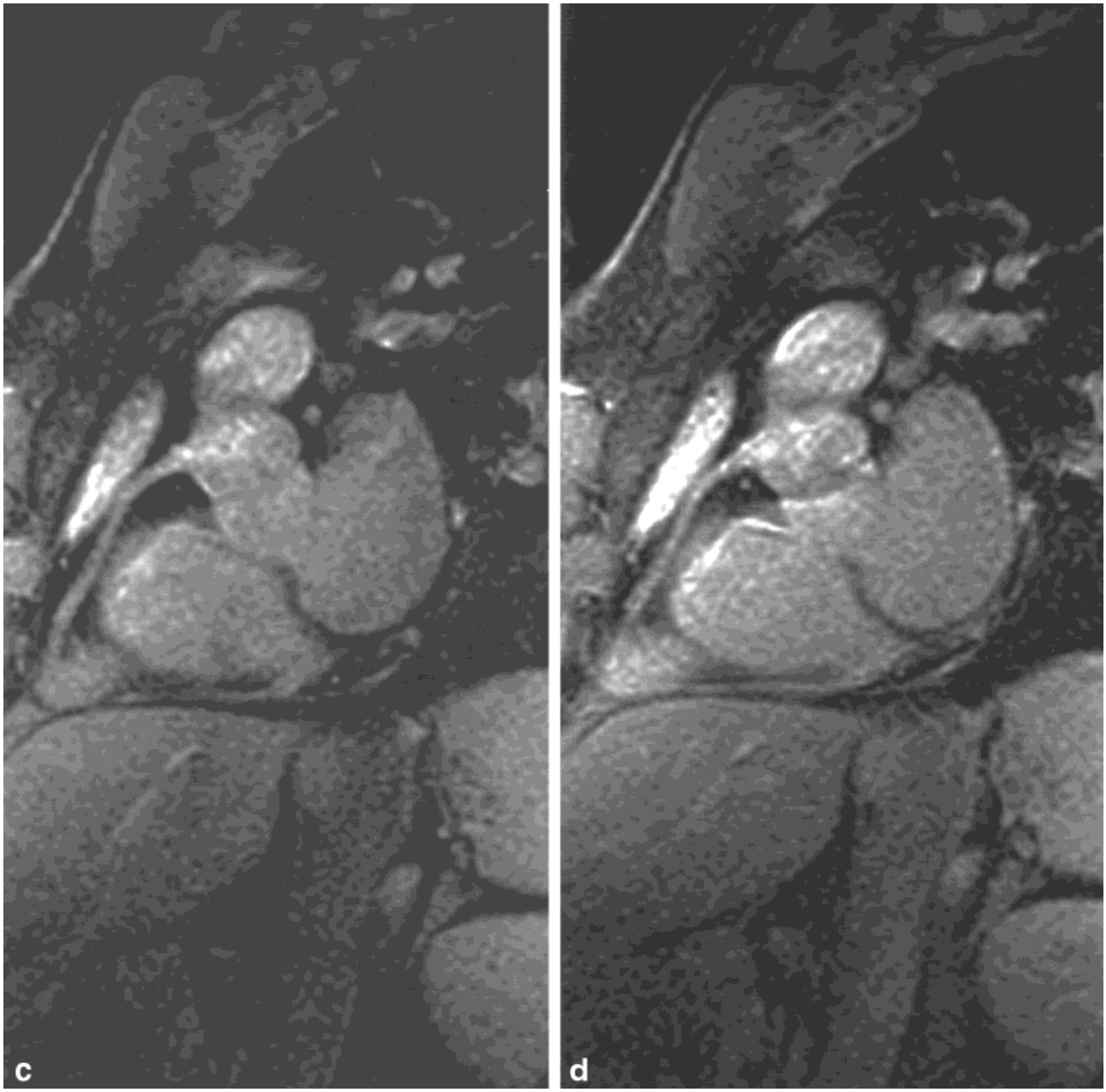

Figure 4. (Continued)

bolus, a feature which provides the possibility of its use in other contrast-enhanced cardiac applications, such as myocardial perfusion imaging. MR SMARTPREP can be used to optimize the patient's breath holding and/or the data acquisition to match contrast arrival. The algorithm provides the added feature of automation that has inherent advantages.

The 2D CMRA sequence used in the study employed sequential phase ordering with the center of k-space sampled during the middle of the 15–22-second image acquisition period. In order to ensure sufficient advance notice of the contrast bolus arrival to synchronize the central k-space views with arterial enhancement, the monitoring volume was placed in the right ventricle (Fig. 1). An improvement to this method would be the modification of the pulse sequence for centric phase ordering, whereby the central k-space data is acquired during the beginning of the imaging period. This would enable the placement of the monitoring volume further "downstream" from the right ventricle and in closer proximity to the coronary arteries (e.g., left ventricle, ascending aorta, or aortic arch). In the current study, all subjects were healthy volunteers. In a patient population, however, significant variations in circulatory time (4) can exist (e.g., a patient with congestive heart failure with slow flow). Centric phase ordering would enable improved placement of the monitor volume closer to the coronary arteries, thereby reducing the intervening vascular territory between the monitor volume and coronary arteries and diminishing potential errors related to circulatory time variations.

Although the experience with Gd-enhanced CMRA is preliminary and the ideal technique (i.e., dose, injection rate, pulse sequence parameters, etc.) has yet to be determined, there appears to be sufficient data to support the use of contrast media for coronary MRA. The vascular signal improvements generated by contrast media enable the opportunities to increase receiver bandwidth, thereby reducing sequence TR and overall scan time, and to acquire higher spatial resolution images for the same scan time. The main disadvantage of extracellular contrast agents, as shown in this study, was diminished visualization of the distal RCA over time, ostensibly due to the leakage of contrast media into the surrounding tissues (increasing background signal and diminishing potential arterial CNR). The use of arterial-phase imaging will reduce the contrast dose requirements and can minimize this concern. Intravascular contrast agents (i.e., blood pool agents), which have diminished extravascular leakage and a prolonged duration of intravascular enhancement, theoretically may be better suited for imaging the coronary arteries than currently available extracellular contrast agents. However, the threefold improvements in arterial CNR that were achieved using single-dose arterial-phase vessel-tracking CMRA in this study compare very favorably with the up to twofold CNR improvements reported by Stillman et al. (23) and Taylor et al. (24) on delayed-phase (steady-state) CMRA imaging with ultrasmall superparamagnetic iron oxide contrast agent and NC100150 injection, respectively. Clearly, additional clinical investigation is required for the determination of the exact role and type of contrast media that ultimately will be recommended for coronary MRA.

REFERENCES

1. Prince MR, Yucel EK, Kaufman JA, Harrison DC, Geller SC. Dynamic gadolinium-enhanced three-dimensional abdominal MR arteriography. J Magn Reson Imaging 1993;3:877–881.
2. Prince MR. Gadolinium-enhanced MR aortography. Radiology 1994;191:155–164.
3. Snidow JJ, Johnson MS, Harris VJ, et al. Three-dimensional gadolinium-enhanced MR angiography for aortoiliac inflow assessment plus renal artery screening in a single breath hold. Radiology 1996; 198:725–732.
4. Earls JP, Rofsky NM, DeCorato DR, Krinsky GA, Weinreb JC. Breath-hold single-dose gadolinium-enhanced three-dimensional MR aortography: usefulness of a timing examination and MR power injector. Radiology 1996;201:705–710.
5. Krinsky GA, Rofsky NM, DeCorato DR, et al. Thoracic aorta: comparison of gadolinium-enhanced three-dimensional MR angiography with conventional MR imaging. Radiology 1997;202:183–193.
6. Meaney JFM, Weg JG, Chenevert TL, Stafford-Johnson D, Hamilton BH, Prince MR. Diagnosis of pulmonary embolism with magnetic resonance angiography. N Engl J Med 1997;336:1422–1427.
7. Isoda H, Takehara Y, Isogai S, et al. Technique for arterial-phase contrast-enhanced three-dimensional MR angiography of the carotid and vertebral arteries. Am J Neuroradiol 1998;19:1241–1244.
8. Hany TF, McKinnon GC, Leung DA, Pfammatter T, Debatin JF. Optimization of contrast timing for breath-hold three-dimensional MR angiography. J Magn Reson Imaging 1997;7:551–556.
9. Lee VS, Rofsky NM, Krinsky GA, Stemerman DH, Weinreb JC. Single-dose breath-hold gadolinium-enhanced three-dimensional MR angiography of the renal arteries. Radiology 1999;211:69–78.
10. Foo TKF, Saranathan M, Prince MR, Chenevert TL. Automated detection of bolus arrival and initiation of data acquisition in fast, three-dimensional, gadolinium-enhanced MR angiography. Radiology 1997;203:275–280.
11. Goldfarb JW, Edelman RR. Coronary arteries: breath-hold, gadolinium-enhanced, three-dimensional MR angiography. Radiology 1998;206:830–834.
12. Kessler W, Laub G, Achenbach S, Ropers D, Moshage W, Daniel WG. Coronary arteries: MR angiography with fast contrast-enhanced three-dimensional breath-hold imaging—initial experience. Radiology 1999;210:566–572.
13. Duerinckx AJ. Coronary MR angiography. Magn Reson Imaging Clin N Am 1996;4:361–418.
14. Foo TKF, Ho VB, Hood MN. Vessel-tracking: prospective adjustment of section-selective MR angiographic locations for improved coronary artery visualization over the cardiac cycle. Radiology 2000;214:283–289.
15. Ho VB, Foo TKF. Optimization of gadolinium-enhanced magnetic resonance angiography using an automated bolus-detection algorithm (MR SMARTPREP). Invest Radiol 1998;33:515–523.
16. Edelman RR, Manning WJ, Burstein D, Paulin S. Coronary arteries: breath-hold MR angiography. Radiology 1991;181:641–643.
17. Meyer CH, Hu BS, Nishimura DG, Macovski A. Past spiral coronary artery imaging. Magn Reson Med 1992;28:202–213.
18. Manning WJ, Li W, Edelman RR. A preliminary report comparing magnetic resonance coronary angiography with conventional angiography. N Engl J Med 1993;328:828–832.
19. Pennell DJ, Keegan J, Firmin DN, Gatehouse PD, Underwood SR, Longmore DB. Magnetic resonance imaging of coronary arteries: technique and preliminary results. Br Heart J 1993;70:315–326.
20. Duerinckx AJ, Urman MK. Two-dimensional coronary MR angiography: analysis of initial clinical results. Radiology 1994;193:731–738.
21. Sakuma H, Caputo GR, Steffens JC, et al. Breath-hold MR cine angiography of coronary arteries in healthy volunteers: value of multiangle oblique imaging planes. Am J Roentgenol 1994;163: 533–537.
22. Brittain JH, Hu BS, Wright GA, Meyer CH, Macovski A, Nishimura DG. Coronary angiography with magnetization-prepared T2 contrast. Magn Reson Med 1995;33:689–696.
23. Stillman AE, Wilke N, Li D, Haacke EM, McLachlan S. Ultrasmall superparamagnetic iron oxide to enhance MRA of the renal and coronary arteries: studies in human patients. J Comput Assist Tomogr 1996;20:51–55.
24. Taylor AM, Panting JR, Keegan J, et al. Safety and preliminary findings with the intravascular contrast agent NC100150 injection for MR coronary angiography. J Magn Reson Imaging 1999;9:220–227.